


# A Novel Approach for Developing Smart Cotton Fabric with Dynamic Breathability and Easy Care Features

Nazife Korkmaz Memiş  0000-0003-1605-0670

Sibel Kaplan  0000-0002-7247-135X

Süleyman Demirel University, Engineering Faculty, Textile Engineering Department, Isparta, Türkiye

**Corresponding Author:** Nazife Korkmaz Memiş, nazifekorkmaz@sdu.edu.tr

## ABSTRACT

In this study, cotton fabrics were treated with temperature-water responsive nanocomposites consisting of shape memory polyurethane (SMPU) and cellulose nanowhiskers (CNWs) for smart crease recovery/retention functions besides breathability. The smart crease recovery/retention functions were determined in air/water at different temperatures and relative humidities simulating laundry and drying processes. Smart breathability function was tested by water vapour permeability tests under different temperatures-relative humidities and air permeability tests at different fabric temperatures. Physical-mechanical properties and washing fastness properties were also investigated. Fourier-transform infrared (FT-IR) and scanning electron microscope (SEM) analyses confirm the SMPU-CNW nanocomposite presence on fabric. Test results show that the treated cotton fabrics have not only dual responsive permeability as a result of dynamic pore structure, but also dynamic crease recovery/retention with enhanced mechanical properties. It is thought that suggested method can contribute to both ecological and economic aspects of sustainability as a result of less energy and polymer consumptions besides smart comfort enhancement and mechanical functions.

## 1. INTRODUCTION

Cotton is one of the most commonly used textile materials for garments worldwide by virtue of its comfort, hydrophilicity, mechanical strength, softness, availability, cost competitiveness, and biocompatibility attributes [1]. Nevertheless, practical usage of pure cotton in garments is restricted by wrinkle and crease tendencies, a disadvantage sourced from slippage movement of the cellulose molecular chains during usage and/or repetitive laundering [2]. Wrinkle and crease tendency of the garments, associated with easy care properties [3], causes a costly and time-consuming ironing process and deterioration of aesthetic appearance during wearing [4]. Recently, expectations of consumers about multi-functionality including easy-care, low maintenance, clothing comfort features, and sustainability issues have increased, especially with COVID-19 pandemic and recent natural events. Correspondingly, crease recovery of the garment, namely, the ability of a fabric to recover from fold deformation, is a desired property especially after laundry cycles. There are also some end uses such as pleating of a garment part (skirt, trouser etc.), where crease retention,

namely, the ability of a fabric to maintain folded appearance, is required [5].

To achieve easy-care performance, especially for crease recovery and retention, different commercial finishing methods and chemicals were developed such as formaldehyde-based easy-care finishes (dimethyloldihydroxy-ethylene urea-DMDHEU) [6], ether derivatives of DMDHEU [7], formaldehyde-free finishes with polycarboxylic acids (1,2,3,4-butane tetracarboxylic acid, citric acid, maleic acid, succinic acid etc.) [8], carboxyl polyaldehyde sugars [9] applied by finishing treatment, foaming [1], and sol-gel technology [10]. But these commercial finishing chemicals and methods have problems with formaldehyde release, a probable human carcinogen, during manufacturing, wearing, and storage [11]. Moreover, other disadvantages of these applications are strength loss [12], poor comfort [13], deterioration in fabric hand [14], high cost [15], and colour changes [16]. The mentioned concerns and disadvantages motivated researchers to develop multifunctional, garments with smart comfort and easy care features while providing

**To cite this article:** Korkmaz Memiş N, Kaplan S. 2023. A novel approach for developing smart cotton fabric with dynamic breathability and easy care features. *Tekstil ve Konfeksiyon*, 33(3), 238-248.

sustainability during production and usage periods by using environmentally non-hazardous materials and single-stage finishing procedures [1].

An alternative smart method by using shape memory polymers (SMPs) was suggested to obtain novel shape memory effect upon body temperature, home laundry, steaming, and hot wind tumble drying processes which enables environmentally adoptable crease recovery and retention behaviours [17-21], dimensional stability, pattern keeping and bagging recovery [22-25]. Among the reported SMPs, thermally responsive shape memory polyurethane (SMPU) has paved the way for developing smart garments which have adaptability to dynamic environmental and body physiological changes in the form of films [26-28], fiber/yarn to produce fabrics [29-44], fabric coating/finishing applications [45-52]. Despite obtained smart thermal comfort features based on dynamic permeability [52], SMPU has not achieved much commercial adoption in textile processing because of the disadvantages such as the necessity of excessive polymer concentration for sufficient shape memory effect leading to poor fabric hand [53], insufficient response time, and high activation temperature. Besides, temperature and moisture/water have a decisive effect on both human physiological phenomena affecting thermal comfort besides textile production and end-use parameters [25]. To tackle the highlighted issues, simultaneous temperature and water/moisture responsive materials have been developed by modifying SMPU with hydrophilic nanoparticles such as CNWs [54]. SMPU-CNW nanocomposites enable water-responsive shape memory effect depending on the plasticization and percolation network formed by CNWs whose hydrogen bonds can be reversibly regulated by water molecules [55-58] beside temperature-induced shape memory effect originally existing in SMPU. These nanocomposites were applied to wool [24, 52, 53] and polyester fabrics [25] as finishing applications and the results are convincing for dynamic crease recovery/retention and porosity changes of fabrics enabling smart breathability. In this context, mentioned dual smart function of SMPU-CNW nanocomposites may be a tool for crease recovery and retention functions during standard laundry and drying procedures without the need for ironing besides smart permeability in dynamic conditions. A single stage of SMPU-CNW nanocomposite finishing application can enhance both thermal comfort and end-use performances while decreasing environmental impacts of the product.

Therefore, in this study, cotton fabrics were treated with nanocomposite solutions prepared by modification of SMPU with CNWs for smart crease recovery and retention functions under temperature or moisture environments (laundry and tumble drying processes) besides smart permeability with dynamic porosity stimulated by the temperature and relative humidity of the body/environment. Moreover, physical-mechanical properties (weight, thickness, bending rigidity, and strength) and washing fastness properties were also evaluated to determine the performance and formability of the treated fabrics.

## 2. MATERIAL AND METHOD

### 2.1 Material

100% cotton woven fabric with an areal density of 117 g/m<sup>2</sup>, yarn density of 58 warp/cm and 38 weft/cm, was kindly supplied by Söktaş Group, Turkey. Temperature and water-responsive nanocomposite suspensions were prepared by using commercial SMPU (SMP Technologies Inc., Japan) (MM-3520, pellet type) having appropriate  $T_{glass\ transition}$  (g) of 32°C [53] as matrix/thermo-responsive switch and CNWs (Grafen Co, Turkey) (150-200 nm length, 20 nm width, and 98.98% crystallinity) as water/humidity responsive switch. Homogenous dispersion of hydrophilic CNWs in a hydrophobic SMPU matrix was ensured by using a non-ionic surfactant (Tween®80, Sigma Aldrich, USA). N, N-dimethylformamide (DMF) (Sigma Aldrich, USA) was used as the solvent. A commercial polyether type polyurethane (Pulcra HPU®, Pulcra Chemicals) without shape memory function, was used as a control finishing agent for comparison. Before the finishing process, cotton fabric was washed 5 times according to TS EN ISO 6330:201, followed by drying at room temperature.

### 2.2 Method

#### 2.2.1 Nanocomposite treatment onto cotton fabrics

A series of temperature and water-responsive nanocomposite suspensions were prepared by nanoreinforcing 10 wt% SMPU-DMF solutions with CNWs (5, 10, and 20 wt% of SMPU) in DMF with Tween®80 at 1:2 w/w of the nanoparticle by mixing two aqueous suspensions homogeneously under ultrasonic stirring for 1 h. After that, cotton fabrics were impregnated with these nanocomposite solutions at an average pick-up ratio of 90% by pad-dry-cure process at a speed of 2 m/min and pressure of 3 bars on the foulard, dried at 85°C for 3 min and cured at 120°C for 2 min. Moreover, cotton fabrics were treated with Pulcra HPU® according to the manufacturer's recommendation at 8 wt% concentration, dried at 120°C for 3 min and cured at 170°C for 30 s. The treated cotton fabrics were coded as CO-SMPU-CNW<sub>x</sub> where x represents CNW concentration.

#### 2.2.2 Characterizations

Presence of the SMPU-CNW nanocomposite and surface morphology of the fabrics were detected using a SEM (Fei Quanta FEG 250, Thermo Scientific) with 20 kV and 10 µA at high magnification of up to 2500 for textile fabrics. Elemental content of the fabrics was investigated by X-ray spectroscopy (EDX) analysis. Spectroscopic analyses of the polymers and fabrics were carried out on KBr disks by using an FT-IR spectroscopy instrument (Perkin Elmer Spectrum BX) with 4 cm<sup>-1</sup> resolution, 2 cm<sup>-1</sup> intervals, and 16 scan numbers in the range of 400-4000 cm<sup>-1</sup>. Physical (weight, thickness) and mechanical (bending rigidity, tear strength) features were determined according to TS 251:2008, ASTM D 1777-96, ASTM D 1388-92:2002, and ISO 13937-2 standards, respectively to identify effects of the treatments on fabric properties.



For determining dynamic permeability function, water vapour permeability (WVP) of the fabrics was measured regarding the standard ASTM E96-80 with plastic cups. Tests were conducted at different ambient temperatures (20°C, 40°C, and 65°C) and relative humidities (20%, 40%, 65%, and 80% for constant temperature of 20°C) with three replicates. To visualize the change trends of permeability with temperature and moisture, ratios of WVP values for different temperatures and relative humidity values ( $WVP_{65^\circ C}/WVP_{20^\circ C}$ ,  $WVP_{40^\circ C}/WVP_{20^\circ C}$ ,  $WVP_{80\%}/WVP_{20\%}$ ,  $WVP_{65\%}/WVP_{20\%}$  etc.) were also calculated. Air permeability was also tested according to ASTM D737-04:2012 at different fabric temperatures with ten replicates. Selected fabric temperatures (20°C, 40°C, and 65°C) were arranged with a hotplate and controlled by a thermal camera (Fluke Ti100 Thermal Imager). Smart crease recovery and retention functions, an indicator of the shape recovery ability, were carried out in different media (air and water at different temperatures and relative humidity) simulating laundry and drying processes according to AATCC 66:1998 by angle measurements. The test procedure was illustrated in Figure 1 and explained in the following steps:

(i) **Evaluation of original shape:** First, the flat original shape for crease recovery (Figure 1(a)) was prepared by ironing both sides of the samples for 30 s at 120°C with 100 g/m<sup>2</sup> pressure then fixing at 120°C for 2 min. The creased original shape for retention (Figure 1(b)) was also prepared by folding the samples, then ironing both sides of folded samples for 30 s at 120°C with 100 g/m<sup>2</sup> pressure and fixing at 120°C for 2 min. Subsequently, the original angles of the flat ( $\theta_{original}=180^\circ$ ) and creased ( $\theta_{original}=0^\circ$ ) fabrics (40 mmx15 mm) on both warp and weft directions were measured.

(ii) **Shape deformation:** The samples were then pressed with 100 g/m<sup>2</sup> pressure for 24 h for temporary shapes (creased samples for crease recovery ( $\theta_{pressed, load}=0^\circ$ ) and

flat samples for crease retention ( $\theta_{pressed, load}=180^\circ$ ). Then, all of the samples were stuck on L-shaped hangers.

(iii) **Recovery process:** Recovery abilities were tested in water and dry air for 5 min and 30 min, respectively at 20°C, 40°C, and 65°C to simulate laundry and drying conditions. Recovery abilities were tested also at different relative humidity values (20%, 40%, and 65%) for a constant temperature of 20°C. For the shape recovery process in water media, the hangers with samples were immersed in a water bath at temperatures of 20°C, 40°C, and 65°C for 5 min. Then, samples were conditioned within a drying frame for 24 h at 65% RH, 20°C. For the shape recovery process in air and relative humidity media, the hangers with the samples were kept in the oven for 30 min under the specified temperature and humidity conditions.

(iv) **Evaluation of shape recovery:** The smart crease recovery and retention performances were determined by angle measurements in the final state ( $\theta_{final}$ ) and ratios were calculated according to Equation (1). In each case, the average warp and weft recovery angles and the sum of the recovery angle from the warp and weft were calculated.

$$C_r = \frac{\theta_{pressed, load} - \theta_{final}}{\theta_{pressed, load} - \theta_{original}} \times 100 \quad (1)$$

For determining the washing fastness of the treated fabrics, the samples were washed repeatedly according to TS EN 20105-C06:2001/A2S program at 40°C for 30 min by using a washing machine (James H. Heal, Gyrowash Model 415). The samples were washed 1, 5, 10, and 20 cycles in an aqueous solution having a liquor ratio of 1:50 with a 4 g/L of ECE standard detergent solution and then the presence of nanocomposite material in the fabric structure after washing was determined by weight changes according to Equation (2).

$$W_L (\%) = \frac{W_0 - W_1}{W_0} \times 100 \quad (2)$$

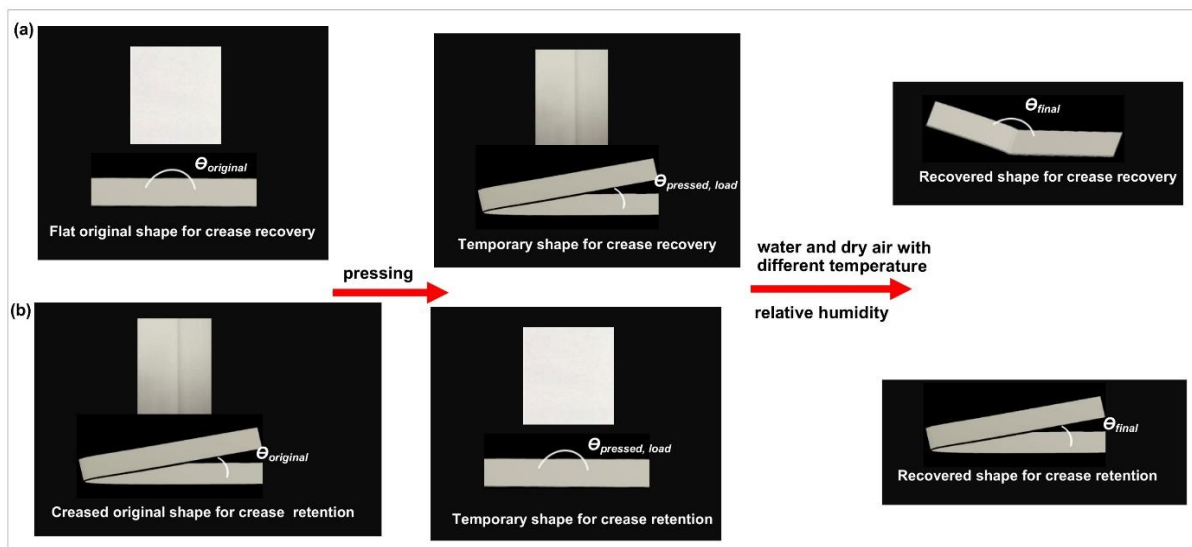


Figure 1. The test procedure of smart crease recovery and retention based on shape memory function



Where  $W_L$ ,  $W_0$ , and  $W_I$  are the weight change, weights of the samples before and after washings, respectively.

SPSS Statistics 22.0 for Windows statistical software (IBM, Armonk, USA) was used to analyse test results statistically. Univariate and Multivariate analysis of variance (MANOVA) at 95% confidence level were conducted to determine the effect of finishing agent type, media, and temperature on the breathability and crease recovery/ retention characteristics, respectively. Parameters were evaluated statistically also with Univariate Analysis of Variance within groups. Student-Newman-Keuls (SNK) tests were used to examine the differences among the measured fabric parameters.

### 3. RESULTS AND DISCUSSION

#### 3.1 Morphology and Elemental Analysis of Cotton Fabrics

In order to investigate the presence of nanocomposite treatment, fabric morphological change, and elemental content, SEM analysis was performed. SEM images and EDX spectra of the selected samples were given in Figure 2. From Figure 2(a)-(b), it can be seen that, the raw sample demonstrates the characteristic convolution structure and smooth surface of the cotton fiber as expected. As shown in Figure 2(c)-(d), Pulcra HPU solution, polyurethane without shape memory property, did not form a film layer on the surface of the fibers. Besides, for the SMPU and also SMPU-CNW nanocomposite treated fabrics, fiber/fabric surfaces were covered with relatively uniform, smoother, and thicker coatings. Moreover, SMPU and SMPU-CNW nanocomposites filled the gaps between the fibers, and bridged the adjacent fibers through adhesion providing fiber-fiber bonding. The nanoparticle distribution on the cotton fabric surface and increased thickness for SMPU-CNW nanocomposite treated fabrics increasing with CNW concentration (e.g. CO-SMPU-CNW20) can be realized in Figure 2(g)-(j).

According to EDX spectra, giving idea about the elemental contents of the investigated fabrics (Figure 2), 54.76% C and 45.24% O elements were detected on the surface of the raw samples. The finishing treatments with Pulcra-HPU, SMPU, and SMPU-CNW nanocomposites caused a decrease in the O/C ratio, an indicator of better wettability, as compared to the raw cotton fabric (0.83). Pulcra-HPU treated fabrics had a higher O/C ratio (0.80) due to the hydrophilic nature of the commercial polyurethane polymer used when compared with the ones treated with SMPU (0.72) and the SMPU-CNW nanocomposites (0.73). Although a small difference, the O/C ratios of SMPU-CNW nanocomposite and SMPU-treated fabrics demonstrate an enhancement in wettability of the fabrics that can be attributed to the hydrophilic nature of CNW particles.

FT-IR analysis was conducted to determine the chemical structures and interactions of the polymers with cotton fabric. FT-IR spectrums of the polymers, raw, and treated

cotton fabrics were given in Figure 3. According to FT-IR spectrums in Figure 3;

- ✓ The commercial polyurethane (Pulcra HPU) and SMPU showed their characteristic bands. Pulcra-HPU exhibited peaks at  $3435\text{ cm}^{-1}$  (-NH absorption peak) and  $1102\text{ cm}^{-1}$  (-C-O-C-) (Figure 3(b)). SMPU exhibited peaks at  $3449\text{ cm}^{-1}$  (urethane stretching vibration),  $2861\text{ cm}^{-1}$  and  $2927\text{ cm}^{-1}$  (-CH<sub>2</sub> stretching),  $1463$ ,  $1406$ ,  $1345$ , and  $1294\text{ cm}^{-1}$  (other modes of -CH<sub>2</sub> vibrations),  $1737\text{ cm}^{-1}$  (C=O stretching), and  $1544\text{ cm}^{-1}$  (-NH), and  $1051\text{ cm}^{-1}$  (-C<sub>2</sub>H<sub>4</sub>-O-C<sub>2</sub>H<sub>4</sub>- ether group) [24, 25, 52, 53] (Figure 3(d)).
- ✓ When the fabric-polymer interactions were evaluated according to FT-IR spectrums, there are no sharp peaks for Pulcra-HPU treated cotton fabrics since it is present in very small amounts within the fabric structure confirming SEM images. After treatment with Pulcra-HPU, a slight gradual decrease in the intensity of (-OH) stretching band at  $3200\text{-}3400\text{ cm}^{-1}$  of the raw cotton samples due to the interaction between the cellulose (-OH) group and the (-NH) bonds of Pulcra HPU, was observed as expected. This can be evaluated as proof of the Pulcra HPU presence on the fabric surface. Moreover, a transmittance descent of (HNC=O) amide group bands at  $1500\text{ cm}^{-1}$  and carbonyl groups of urea at  $1750\text{ cm}^{-1}$  in the Pulcra-HPU treated fabrics compared to Pulcra-HPU polymer, is another proof of the Pulcra HPU bonding.

On the other hand, the peak at  $1737\text{ cm}^{-1}$  for the SMPU polymer can be attributed to the free urethane (C=O) groups (Figure 3(c)), while the peak at approximately  $1700\text{ cm}^{-1}$  for SMPU treated cotton samples indicates the hydrogen-bonded urethane (C=O) groups [24, 25, 52, 53, 59]. Besides, a decrease in the intensity of (-OH) stretching band in the wavelength range of  $3200\text{-}3400\text{ cm}^{-1}$  was observed after SMPU treatment. This may occur with the reaction of the free isocyanate groups of polyurethane, which may be formed as a result of thermal decomposition with the effect of temperature during the drying and curing processes, and the (-OH) group of cellulose [60]. Furthermore, the decrease of (-OH) in-plane stretching band in the range of  $900\text{-}1200\text{ cm}^{-1}$  for treated fabrics when compared with the raw ones indicates that the SMPU polymer reacts with the (-OH) groups of cotton. Different from the raw cotton fabric, (-CH<sub>2</sub>) stretching peak at  $2975\text{ cm}^{-1}$  and the characteristic (-C<sub>2</sub>H<sub>4</sub>-O-C<sub>2</sub>H<sub>4</sub>-) ether peak at  $1049\text{ cm}^{-1}$  in the treated fabrics (Figure 3(e)) prove the existence of SMPU in the fabric structure. On the other hand, different from SMPU-treated fabrics, SMPU-CNW nanocomposite-treated ones exhibited a broader and more intense peak of hydrogen-bonded urethane (C=O) groups at  $1703\text{ cm}^{-1}$  with the increase of CNW content (Figure 3(f)-(g)). This is an indicator of the SMPU-CNW nanocomposite treatment presence in the cotton fabric structure.





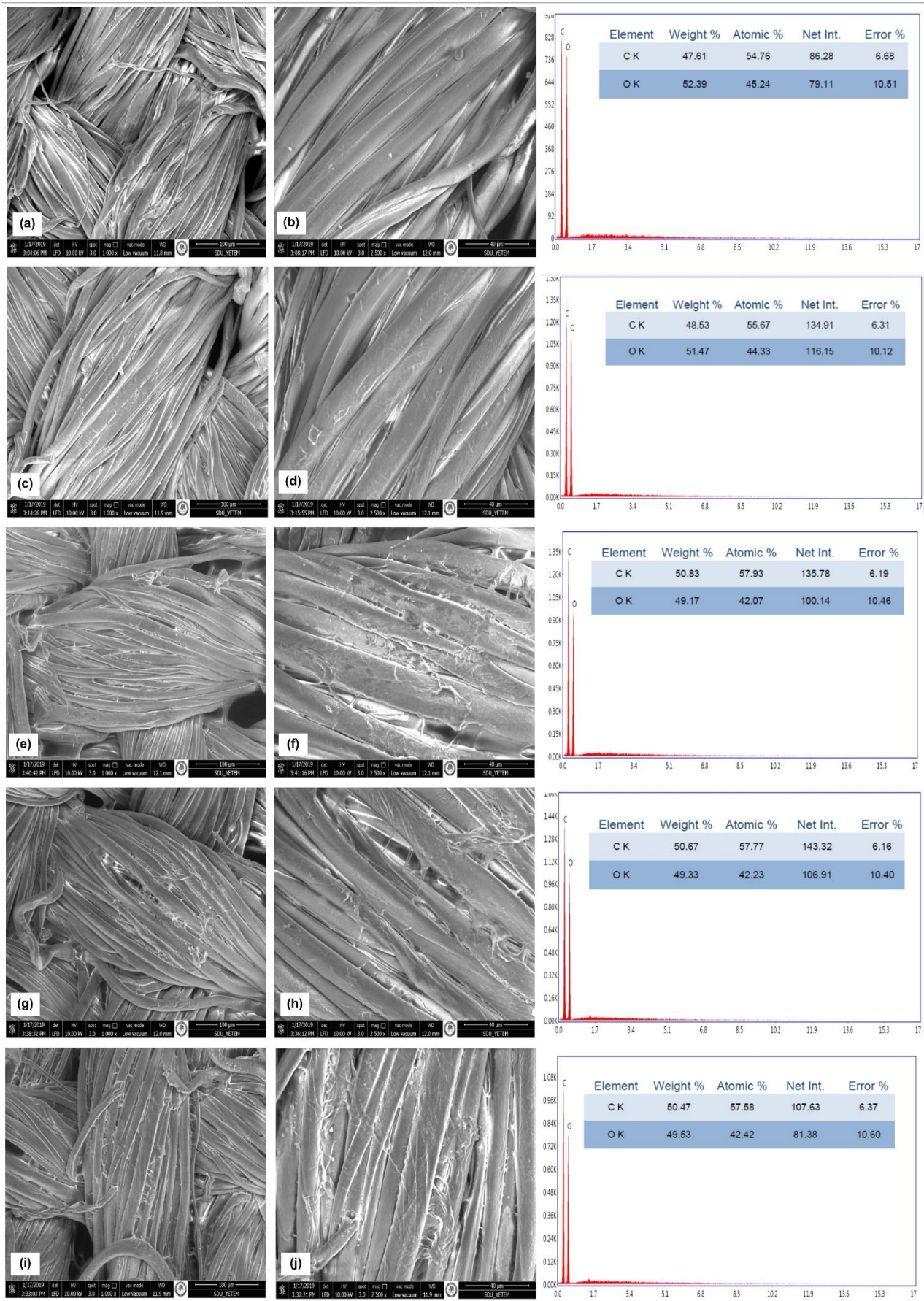


**Figure 2.** SEM images of cotton fabrics at 1000x and 2500x; raw cotton fabric (a, b), CO-Pulcra HPU (c, d), CO-SMPU (e, f), CO-SMPU-CNW5 (g, h), CO-SMPU-CNW20 (i, j)

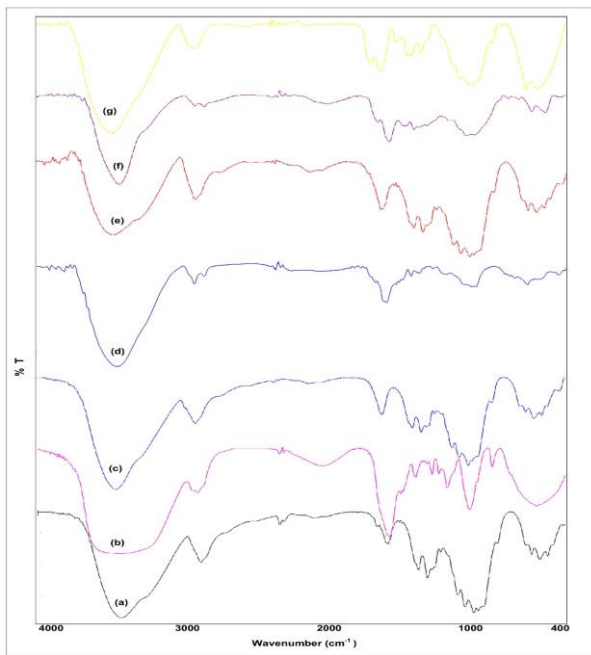


**Figure 3.** FT-IR spectra of raw cotton fabric (a), Pulcra HPU emulsion (b), CO-Pulcra HPU (c), SMPU polymer (d), CO-SMPU (e), CO-SMPU-CNW5 (f), CO-SMPU-CNW20 (g)

### 3.2 Physical and Mechanical Features of Cotton Fabrics

The physical and mechanical features of the cotton fabrics with their statistical analysis results are given in Table 1. According to the results, while SMPU and SMPU-CNW nanocomposite treatments created significant areal density differences proportional to CNW concentration, is not the case for CO-Pulcra HPU. A similar trend was observed for bending rigidity and tear strength properties that SMPU-CNW10 and SMPU-CNW20 fabrics have lower bending rigidities than SMPU-treated ones, a positive result for fabric hand. Statistically insignificant thickness changes with both SMPU (0.27 mm) and SMPU-CNW (0.25 mm) treated fabrics also confirm bending rigidity values. Besides, tensile strength of the fabrics increased by approximately 21.26% compared to the raw ones with SMPU-CNW20 nanocomposite treatment.

### 3.3 Shape Memory Features of Cotton Fabrics

#### 3.3.1 Dynamic water vapour permeability

Water vapour permeability is the main indicator of breathability, affecting the comfort properties of clothing systems besides air permeability in both daily life and extreme conditions. Hence, dynamic WVP or breathability features of the raw and treated cotton fabrics, based on the simultaneous temperature and water/moisture responsive shape memory functions, were measured as well. Univariate ANOVA analysis results show that WVP values changed significantly with the treatment type (CNW concentration), temperature/relative humidity, and two-way interactions of the mentioned parameters ( $p=0.00<0.05$ ), meaning dynamic breathability based on temperature and

water/moisture responsive shape memory function. The WVP values of the fabrics were plotted in Figure 4(a) and Figure 4(b) according to different temperatures and relative humidity values. According to Figure 4(a), at temperatures ( $20^{\circ}\text{C}$ ) below  $T_g$  of SMPU ( $32^{\circ}\text{C}$ ) [53], WVP values of the treated fabrics, especially values of the SMPU and SMPU-CNW nanocomposite treated ones were lower than the raw fabric as expected due to the polymer covering spaces among yarns. When the effect of temperature is considered, there is an apparent increase trend directly proportional to temperature. As in the air permeability, at higher temperatures above  $T_g$  of SMPU ( $40^{\circ}\text{C}$  and  $65^{\circ}\text{C}$ ), Pulcra-HPU treated samples had the minimum WVP value which is significantly different from the other samples. The temperature-responsive performances of the SMPU and SMPU-CNW nanocomposite treatments were apparent for the temperatures above  $T_g$  of SMPU ( $40^{\circ}\text{C}$  and  $65^{\circ}\text{C}$ ) and there are increase trends for all samples, SMPU-CNW20 being the highest. Moreover, increase trends of WVP values calculated from ratios of WVP for different temperatures show that there are surely increase trends for  $\text{WVP}_{40^{\circ}\text{C}}/\text{WVP}_{20^{\circ}\text{C}}$  and  $\text{WVP}_{65^{\circ}\text{C}}/\text{WVP}_{20^{\circ}\text{C}}$  and the maximum increment was for CO-SMPU-CNW20 (5.86 and 13.46, respectively). According to the mentioned results, it can be concluded that, the dynamic WVP feature mainly originates from the fact that SMPU polymer chains act as a smart gate changing pore size and structure reversibly due to temperature-sensitive free volume [61] and micro-Brownian motion [50, 51]. Moreover, adding CNW nanoparticles into the SMPU matrix promotes dynamic water vapor permeability function by the occurrence of additional permanent micro-voids and probable stretching and distorting of hydrogen bonds formed among CNWs with temperature [62].

WVP values differing according to relative humidity values as seen in Figure 4(b), changed significantly with relative humidity and finishing treatment ( $p<0.05$ ), indicating water/moisture-responsive function of the nanocomposite. WVP reached the maximum value for SMPU-CNW20 at 40% relative humidity, a moderate value for a comfortable zone [61]. These findings can be evaluated as an indicator of moisture-sensitive water vapour permeability obtained by strong hydrogen bonding of CNW percolation network which can be broken by moisture molecules [61] within SMPU matrix leading opening of channel for water to pass through. When the mentioned phenomenon occurs, pores form or their number increase for more water vapour transfer. For higher relative humidity levels than 40%, the permeability of all fabric samples decreased as a result of water vapour concentration gradient reduction between the microclimate and environment [63]. It is thought that the mentioned dynamic changes of water vapour permeability values with body/environment temperature and relative humidity could improve thermoregulation by supporting the insulation effect at low temperatures and heat transfer at high temperatures as well as low and high humidity values.





**Table 1.** Physical and mechanical features of the cotton fabrics

Samples	Weight (g/m <sup>2</sup> )	Bending rigidity (mg.cm)	Tear strength (N)	
			Warp	Weft
Raw cotton fabric	117 <sup>a</sup> ±2.05	171.21 <sup>a</sup> ±3.41	4.61 <sup>a</sup> ±0.35	4.12 <sup>a</sup> ±0.19
CO-Pulcra HPU	119 <sup>a</sup> ±0.61	160.45 <sup>a</sup> ±13.27	5.28 <sup>b</sup> ±0.15	4.22 <sup>a</sup> ±0.18
CO-SMPU	121 <sup>b</sup> ±0.03	501.47 <sup>c</sup> ±22.26	5.30 <sup>bc</sup> ±0.10	4.22 <sup>a</sup> ±0.11
CO-SMPU-CNW5	124 <sup>bc</sup> ±1.22	487.55 <sup>c</sup> ±32.88	5.34 <sup>bc</sup> ±0.22	4.58 <sup>b</sup> ±0.45
CO-SMPU-CNW10	126 <sup>c</sup> ±0.40	442.28 <sup>b</sup> ±13.29	5.58 <sup>c</sup> ±0.20	4.61 <sup>b</sup> ±0.26
CO-SMPU-CNW20	127 <sup>c</sup> ±0.23	437.13 <sup>b</sup> ±20.05	5.59 <sup>c</sup> ±0.16	5.18 <sup>c</sup> ±0.06

Note: Superscripts show significant differences among the results ( $p < 0.005$ )

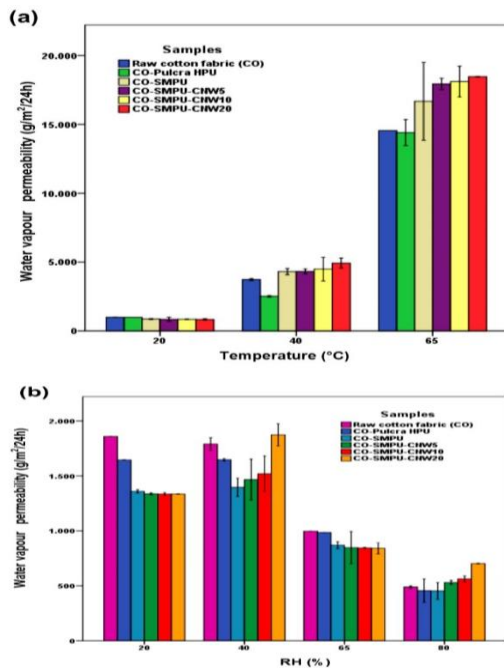


**Figure 4.** Water vapour permeability values according to temperature (a) and relative humidity (b)

### 3.3.2 Dynamic air permeability

Air permeability, the measure of air that the fabric allows to pass through due to its porous structure, facilitates convective heat transfer besides influencing water vapour permeability [64]. This function can be passively improved by fiber and yarn properties, fabric structure, as well as finishing processes by managing the shape and volume of airflow channels within the fabric [65, 66]. The dynamic air permeability results were summarized in Figure 5. According to the results, the air permeability of the raw cotton fabric was 122.66 l/m<sup>2</sup>/s at 20°C and did not change significantly at 40°C and 65°C, as expected. On the other hand, nanocomposite treatment (CNW concentration), temperature and their interactions have statistically significant effects ( $p < 0.05$ ) on air permeability. At temperatures below  $T_g$  of SMPU (32°C), air permeability values of all the treated fabrics were lower than the raw fabric as expected due to the polymer covering spaces among yarns confirming SEM images. However, as the temperature was raised above  $T_g$  of SMPU such as 40°C and 65°C, there were apparent increase trends for SMPU

and especially for SMPU-CNW nanocomposite treated fabrics, proportional to CNW concentration. On the contrary, although not statistically significant ( $p > 0.05$ ), air permeability values of CO-Pulcra HPU decreased with temperature increase due to the polymer structure of Pulcra HPU, which is not temperature sensitive. Air permeability comparisons with the values for 20°C (differences), given in Figure 5(b), supported these results that SMPU-CNW nanocomposite treated fabrics are notably sensitive to temperature. It is clear that adding ceratin amount of CNW nanoparticles into the SMPU matrix promotes dynamic air permeability function by the occurrence of additional permanent micro-voids, increasing in size and in number [67] as a result of probable stretching and distorting of hydrogen bonds formed among CNWs beside free volume increasing of the polymer (SMPU matrix) amorphous phase with temperature. Considering both water and air permeability results, it can be concluded that the adaptive comfort properties in cotton fabrics could be obtained with SMPU-CNW nanocomposite treatment.

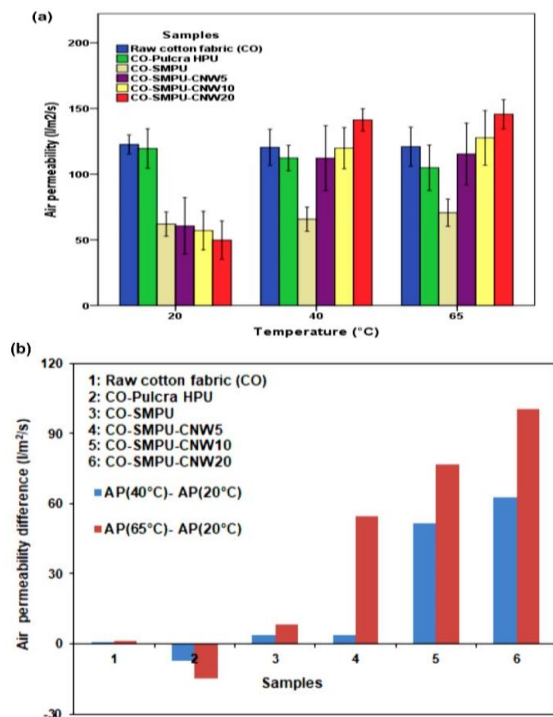


**Figure 5.** Air permeability values (a), change in air permeability values of cotton fabrics according to temperature (b)

### 3.3.3 Smart crease recovery and retention

Fabrics are often subject to repeated crease and bending deformations, like elbow movements, and crease recovery or retention abilities of fabrics are important for end-use and formability of the garments. Crease recovery is always a desired property, especially for natural-fiber fabrics like cotton, which has a higher tendency to crease, and crease retention may be required for some garment formations such as pleated skirts. Thus, the crease recovery and retention functions of the SMPU-treated cotton fabrics were determined under different media simulating home laundering and/or tumble drying without the need for ironing or another extra energy-expending procedure. The crease recovery and retention ratios of the cotton fabrics in air and water media under different temperatures and relative humidity values were presented in Figure 6 and Figure 7, respectively. MANOVA test results show that crease recovery and retention values increased significantly with the treatment type (CNW concentration), temperature/relative humidity, type of test media (water/air), and all double and triple interactions of the mentioned parameters ( $p < 0.05$ ), meaning a smart shape memory function. The crease recovery and retention functions were enhanced for SMPU and SMPU-CNW nanocomposite treated fabrics increasing with CNW concentrations, better than the increment for Pulcra-HPU (Figure 6). CO-SMPU-CNW20 has the highest crease recovery ratio at 65°C; 59.72% in dry air and 88.05% in water. This result showed that cotton fabric crease that occurred during wear conditions can recover better during the laundry process with the dual responsiveness of the SMPU-CNW nanocomposite treatment and a further recovery can be enabled during home drying. Better performance of water than air under the same temperatures can be explained by the higher thermal conductivity of water [18] providing the trigger of shape memory ability. Crease retention results showed a similar trend that CO-SMPU-CNW20 has the highest values such as 68.52% in dry air and 69.44% in water at 65°C, showing an environmental adaptable memory effect that may be a solution for setting pleated skirts. These data imply that shape memory characteristics were imparted to cotton fabric probably through grafting onto or between fibre surfaces, reducing the residual stress in both warp and weft yarns and increasing the elasticity [18]. SMPU and SMPU-CNW nanocomposite distribution on the surface of the cotton fabric/fiber seen in SEM images and FT-IR analyses (grafting SMPU and SMPU-CNW nanocomposite on the fabric surface) supported this assumption. Furthermore, thicker polymer film formation with SMPU-CNW nanocomposites especially at 20% nanoparticle content, as can be seen in SEM images, resulted in recovery/retention enhancement. The thermo-responsive viscoelastic behaviour and molecular mobility of SMPU polymer chain, hence dimensional change of the coated film on fabric/fiber surface resulted in smart crease recovery/retention functions. This thermo-responsiveness

segregates classical wrinkle-free finishes with DMDHEU, polycarboxylic acid etc. from shape memory finish [18, 67]. Probable stretching and distorting of hydrogen bonds among CNWs by temperature in dry air [62] and plasticization based on reversibly regulating hydrogen bonds among CNWs by water/moisture molecules in an aqueous medium are thought to promote smart crease recovery and retention functions. On the other hand, Pulcra HPU solution did not form a film layer on the surface of the fibers and penetrated into the fiber resulting in induced residual strain inside the fibers hence elasticity and also complete recovery [18].

As can be seen in Figure 7, SMPU and SMPU-CNW nanocomposite treated cotton fabrics have higher recovery and retention ratios increasing with CNW concentration and relative humidity but ratios are lower than the ones obtained for temperature in air/water. With relative humidity increasing, the crease recovery and retention functions reached maximum ratios for CO-SMPU-CNW20 (37.5% and 58.80%, respectively). CO-Pulcra HPU has lower crease recovery and retention ratios than raw fabric. Water/moisture responsiveness of the SMPU-CNW nanocomposite finishing process depending on reversibly broken and rebuilt hydrogen bonding among CNWs was confirmed for relative humidity. All these results show that SMPU-CNW nanocomposite treatment can meet the current demand for wrinkle-free/shape adaptable cotton fabric during standard laundry and drying procedures without needing ironing along with smart comfort, acceptable hand and mechanical properties. The conservation of energy with this method contributes to ecological and economic aspects of sustainability besides being functional [68].

In addition, the lifetime of the materials coated onto the textile materials is a crucial property during usage and should be stable and not easily removed from the textiles. Otherwise, the special functions established by the coated materials will be eliminated. Therefore, the washing fastness properties of the treatments were determined by weight loss after several washing cycles. As seen in Figure 8, the maximum weight loss was observed for CO-Pulcra HPU after 1, 5, 10, and 20 washing cycles, reaching up to 6.089%. Raw cotton fabric follows the CO-Pulcra HPU with a weight loss of 5.772%. The small amount of Pulcra HPU treatment on the fabric surface seen in SEM images could not prevent fiber loss with washings. On the other hand, the weight loss with washing decreased for SMPU and SMPU-CNW nanocomposite treated fabrics. For SMPU-CNW nanocomposite treated cotton fabrics, the weight loss changed inversely with CNW concentration and decreased to 1.47% at 20% CNW content. It can be concluded that the washing fastness of the cotton fabric was enhanced with SMPU-CNW nanocomposite treatment probably through grafting of the polymer onto the fiber surface to form inter-fiber and inter-yarn bonds as seen in FT-IR analysis. Lower weight loss after several washings with SMPU-CNW nanocomposite treatment, meaning less microfiber and polymer release to the aqueous environment is another environmental advantage in decreasing chemical footprint.





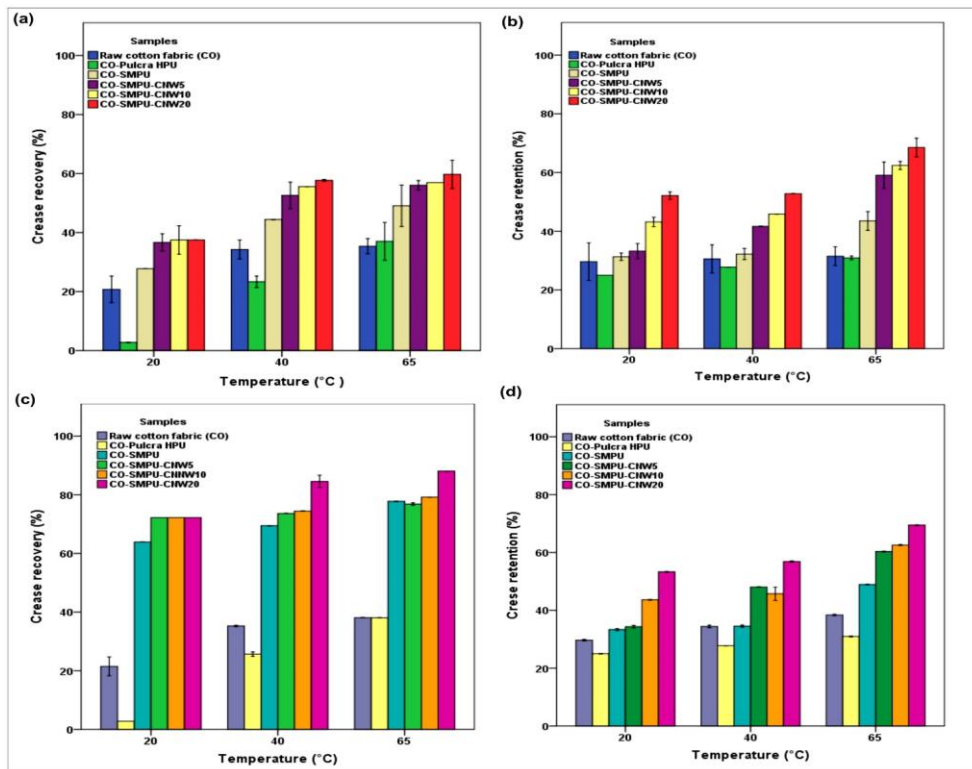


Figure 6. Crease recovery and retention ratios of cotton fabrics at different air (a, b) and water (c, d) temperatures

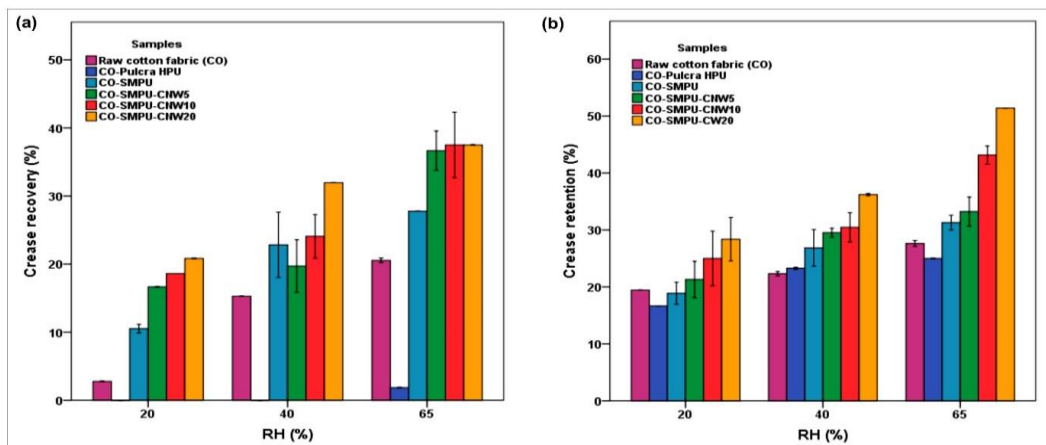


Figure 7. Crease recovery (a) and retention (b) ratios of cotton fabrics at different relative humidity values

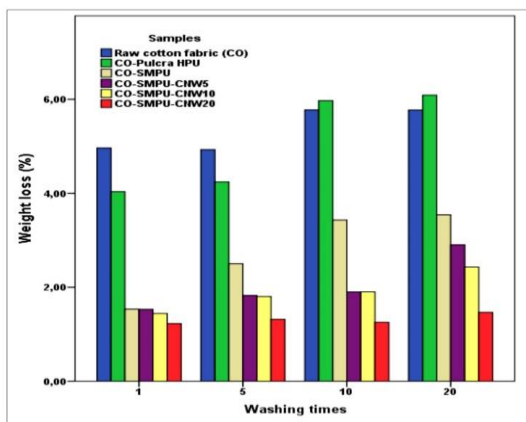


Figure 8. Weight loss of the raw and treated cotton fabrics as a function of washing times

#### 4. CONCLUSION

In this research, cotton fabric with dynamic permeability and multifunctional easy-care features was successfully developed using a simultaneous temperature and water/moisture responsive SMPU-CNW nanocomposite finishing treatment. Results indicated that cotton fabrics with SMPU-based nanocomposite treatments had not only dual responsive shape memory properties providing smart permeability, but also dynamic crease recovery/retention with enhanced or acceptable mechanical properties. It can be concluded that SMPU-CNW nanocomposite structures, especially with 20% CNW content are thought to be suitable materials for smart and multifunctional garments that can be used for both daily and functional clothing such as sports and protective.



Additionally, this method offers a more environmentally friendly approach with less energy and polymer consumption due to non-ironing property and treatment procedures.

## Acknowledgement

This study was funded by the Scientific and Technological Council of Turkey (Project No. 118M228) and Süleyman Demirel University (Project No. 05424-DR-14). Furthermore, the authors would like to express their gratitude to Söktaş Group and also Pulcra Chemicals for fabric and chemical material supply, respectively.

## REFERENCES

1. Sarwar N, Humayoun UB, Nawaz A, Yoon DH. 2021. Development of sustainable, cost effective foam finishing approach for cellulosic textile employing succinic acid/xylitol crosslinking system *Sustainable Materials and Technologies* 30, e00350.
2. Korkmaz N, Alay Aksoy S. 2016. Enhancing the performance properties of ester-cross-linked cotton fabrics using Al<sub>2</sub>O<sub>3</sub>-NPs *Textile Research Journal* 86(6), 636-648.
3. Xiao C, Sun F, Iqbal MI, Liu L, Gao W. 2021. Mechanical characterization of surface wrinkling properties in fibrous sheet materials by facile folding process *Polymer Testing* 97, 107153.
4. Patil NV, Netravali AN. 2020. Multifunctional sucrose acid as a 'green' crosslinker for wrinkle-free cotton fabrics *Cellulose* 27(9), 5407-5420.
5. Lu J, Hu JL, Zhu Y, Liu YJ. 2012. Shape memory finishing of wool fabrics and garments *Advanced Materials Research* 441, 235-238.
6. Harifi T, Montazer M. 2012. Past, present and future prospects of cotton cross-linking: New insight into nano particles *Carbohydrate Polymers* 88(4), 1125-1140.
7. Haule LV, Nambela L. 2022. Sustainable application of nanomaterial for finishing of textile material. In Shanker U, Mustansar Hussain C, Rani M. (Ed.), *Green Nanomaterials for Industrial Applications*. Oxford: Elsevier, 177-206.
8. Wang H, Zhang C, Chu X, Zhu P. 2020. Mechanism of antiwrinkle finishing of cotton fabrics using mixed polycarboxylic acids *International Journal of Polymer Science*. Retrieved from <https://doi.org/10.1155/2020/3876595>.
9. Lou J, Wang D, Fan X. 2022. Preparation, characterization of carboxyl polyaldehyde sugars and application as innovative anti-crease finishing agents for cotton fabric *Journal of Natural Fibers*, 1-8.
10. Arık B, Yavaş A, Avinc, O. 2017. Antibacterial and wrinkle resistance improvement of nettle biofiber using Chitosan and BTCA *Fibres & Textiles in Eastern Europe* 25, 106-111.
11. Mohsin M, Sarwar N, Ahmad S, Rasheed A, Ahmad F, Afzal A, Zafar S. 2016. Maleic acid crosslinking of C-6 fluorocarbon as oil and water repellent finish on cellulosic fabrics *Journal of Cleaner Production* 112, 3525-3530.
12. Kang IS, Yang CQ, Wei W, Lickfield GC. 1998. Mechanical strength of durable press finished cotton fabrics: Part I: Effects of acid degradation and crosslinking of cellulose by polycarboxylic acids *Textile Research Journal* 68(11), 865-870.
13. Xu H, Canisag H, Mu B, Yang Y. 2015. Robust and flexible films from 100% starch cross-linked by biobased disaccharide derivative *ACS Sustainable Chemistry & Engineering* 3(11), 2631-2639.
14. Dadashian F, Montazer M, Ferdowsi S. 2010. Lipases improve the grafting of poly (ethylene terephthalate) fabrics with acrylic acid *Journal of Applied Polymer Science* 116(1), 203-209.
15. Sarwar N, Mohsin M, Bhatti AA, Ahmmad SW, Husaain A. 2017. Development of water and energy efficient environment friendly easy care finishing by foam coating on stretch denim fabric *Journal of Cleaner Production*, 154, 159-166.
16. Qi H, Zhao C, Qing FL, Yan K, Sun G. 2016. Antiwrinkle finishing of cotton fabrics with 5-(Carbonyloxy succinic)-benzene-1, 2, 4-tricarboxylic acid: Comparison with other acids *Industrial & Engineering Chemistry Research* 55(46), 11850-11856.
17. Li YKS. 2006. Evaluation of shape memory fabrics (Master of Philosophy dissertation). Retrieved from/Available from The Hong Kong Polytechnic University Thesis Center.
18. Liu X, Hu J, Murugesu Babu K, Wang S. 2008. Elasticity and shape memory effect of shape memory fabrics *Textile Research Journal* 78(12), 1048-1056.
19. Korkmaz Memiş N, Kaplan S. 2019, November. Improving dynamic crease recovery and retention features of wool fabrics by shape memory nanocomposites. Proceedings of the 17th National 3rd International The Recent Progress Symposium on Textile Technology and Chemistry (137-143), Bursa, Turkey.
20. Korkmaz Memiş N, Kaplan S. 2019, June. Dynamic crease recovery and retention of wool fabric by shape memory polyurethane. Proceedings of the 47th Textile Research Symposium (79-80), Liberec, Czechia.
21. Korkmaz Memiş N. 2020. Textile applications of cellulose nanowhisker reinforced thermo-water responsive polyurethane composite structure (Doctoral dissertation). Retrieved from/ Available from Yök National Thesis Center. (615324)
22. Liu Y, Lu, J, Hu J, Chung A. 2013. Study on the bagging behavior of knitted fabrics by shape memory polyurethane fiber *Journal of the Textile Institute* 104(11), 1230-1236.
23. Korkmaz Memiş N, Kaplan S. 2019, April. Enhancing wool fabric bagging recovery by shape memory polyurethane finishing. Proceedings of the International Congress on Wool and Luxury Fibres – ICONWOOLF 2019 (74-81), Tekirdağ, Turkey.
24. Memiş NK, Kaplan S. 2020. Enhancing wool fabric easy care properties by shape memory polyurethane finishing *AATCC Journal of Research* 7(3), 26-33.
25. Memiş NK, Kaplan S. 2021. Temperature and moisture responsive nanocomposite treated polyester fabric for smart bagging recovery *Indian Journal of Fibre & Textile Research* 46(3), 293-302.
26. Ding XM, Hu JL, Tao XM. 2004. Effect of crystal melting on water vapor permeability of shape-memory polyurethane film *Textile Research Journal* 74, 39-43.
27. Mondal S, Hu JL. 2006. Segmented shape memory polyurethane and its water vapor transport properties *Designed Monomers and Polymers* 9, 527-550.
28. Chen S, Hu J, Liu Y, Liem H, Zhu Y, Meng Q. 2007. Effect of molecular weight on shape memory behavior in polyurethane films *Polymer International* 56, 1128-1134.
29. Zhu Y, Hu J, Yeung LY, Liu Y, Ji F, Yeung KW. 2006. Development of shape memory polyurethane fiber with complete shape recoverability *Smart Materials and Structures* 15(5), 1385.
30. Kaursoin J, Agrawal AK. 2007. Melt spun thermoresponsive shape memory fibers based on polyurethanes: Effect of drawing and heat - setting on fiber morphology and properties *Journal of Applied Polymer Science* 103(4), 2172-2182.
31. Liu Y, Chung A, Hu J, Lv J. 2007. Shape memory behavior of SMPU knitted fabric *Journal of Zhejiang University-Science A* 8(5), 830-834.



32. Meng Q, Hu J, Zhu Y, Lu J, Liu Y. 2007. Morphology, phase separation, thermal and mechanical property differences of shape memory fibres prepared by different spinning methods *Smart Materials and Structures* 16(4), 1192.
33. Zhu Y, Hu J, Yeung LY, Lu J, Meng Q, Chen S, Yeung KW. 2007. Effect of steaming on shape memory polyurethane fibers with various hard segment contents *Smart Materials and Structures* 16(4), 969.
34. Jing L, Hu J. 2010. Study on the properties of core spun yarn and fabrics of shape memory polyurethane *Fibres & Textiles in Eastern Europe* 18(4), 39-42.
35. Liu Y, Lu J, Hu J, Chung A. 2013. Study on the bagging behavior of knitted fabrics by shape memory polyurethane fiber *Journal of the Textile Institute* 104(11), 1230-1236.
36. Yang Q, Li G. 2014. Investigation into stress recovery behavior of shape memory polyurethane fiber *Journal of Polymer Science Part B: Polymer Physics* 52(21), 1429-1440.
37. Budun S, İlgören E, Erdem R, Yüsek M. 2016. Morphological and mechanical analysis of electrospun shape memory polymer fibers *Applied Surface Science* 380, 294-300.
38. Aslan S, Kaplan S. 2018. Thermomechanical and shape memory performances of thermo-sensitive polyurethane fibers *Fibers and Polymers* 19(2), 272-280.
39. Sáenz-Pérez M, Bashir T, Laza JM, García-Barrasa J, Vilas JL, Skrifvars M, León LM. 2019. Novel shape-memory polyurethane fibers for textile applications. *Textile Research Journal* 89(6), 1027-1037.
40. Gupta P, Garg H, Mohanty J, Kumar B. 2020. Excellent memory performance of poly (1, 6-hexanediol adipate) based shape memory polyurethane filament over a range of thermo-mechanical parameters *Journal of Polymer Research* 27(12), 1-13.
41. Ni QQ, Guan X, Zhu Y, Dong Y, Xia H. 2020. Nanofiber-based wearable energy harvesters in different body motions *Composites Science and Technology* 200, 108478.
42. Tonndorf R, Aibibu D, Cherif C. 2020. Thermoresponsive shape memory fibers for compression garments *Polymers* 12(12), 2989.
43. Guan X, Xia H, Ni QQ. 2021. Shape memory polyurethane - based electrospun yarns for thermo - responsive actuation *Journal of Applied Polymer Science* 138(24), 50565.
44. Shi Y, Chen H, Guan X. 2021. High shape memory properties and high strength of shape memory polyurethane nanofiber-based yarn and coil *Polymer Testing* 107277.
45. Cho J.W, Jung YC, Chun BC, Chung YC. 2004. Water vapor permeability and mechanical properties of fabrics coated with shape - memory polyurethane *Journal of Applied Polymer Science* 92(5), 2812-2816.
46. Ye qiu L, Jinlian H, Yong Z, Zhuohong Y. 2005. Surface modification of cotton fabric by grafting of polyurethane *Carbohydrate Polymers* 61(3), 276-280.
47. Liem H, Yeung LY, Hu JL. 2007. A prerequisite for the effective transfer of the shape-memory effect to cotton fibers *Smart Materials and Structures* 16(3), 748.
48. Mondal S, Hu JL. 2007. Water vapor permeability of cotton fabrics coated with shape memory polyurethane *Carbohydrate Polymers* 67(3), 282-287.
49. Dong ZE, Jinlian H, Liu Y, Liu Y, Kuen Chan L. 2008. The performance evaluation of the woven wool fabrics treated with shape memory polymers *International Journal of Sheep and Wool Science* 56(1), 8-18.
50. Bao LH, Ma HT. 2017. Preparation of temperature-sensitive polyurethanes based on modified castor oil *Fibres & Textiles in Eastern Europe* 25, 34-39.
51. Jahid MA, Hu J, Wong K, Wu Y, Zhu Y, Sheng Luo HH, Zhongmin D. 2018. Fabric coated with shape memory polyurethane and its properties *Polymers* 10(6), 681.
52. Memiş NK, Kaplan S. 2020. Wool fabric having thermal comfort management function via shape memory polyurethane finishing *The Journal of The Textile Institute* 111(5), 734-744.
53. Korkmaz Memiş N, Kaplan S. 2020. Dual responsive wool fabric by cellulose nanowhisker reinforced shape memory polyurethane *Journal of Applied Polymer Science* 137(19), 48674.
54. Xia L, Yang F, Wu H, Zhang M, Huang Z, Qiu G, Xin F, Fu W. 2020. Novel series of thermal-and water-induced shape memory Eucommia ulmoides rubber composites *Polymer Testing* 81, 106212.
55. Luo H. 2012. Study on stimulus-responsive cellulose-based polymeric materials (Doctoral dissertation). Retrieved from/Available from The Hong Kong Polytechnic University Thesis Center.
56. Tan L, Hu J, Ying Rena K, Zhu Y, Liu P. 2017. Quick water - responsive shape memory hybrids with cellulose nanofibers *Journal of Polymer Science Part A: Polymer Chemistry* 55(4), 767-775.
57. Wang Y, Cheng Z, Liu Z, Kang H, Liu Y. 2018. Cellulose nanofibers/polyurethane shape memory composites with fast water-responsivity *Journal of Materials Chemistry B* 6(11), 1668-1677.
58. Zhu Y, Hu J, Luo H, Young RJ, Deng L, Zhang S, Fan Y, Ye. 2012. Rapidly switchable water-sensitive shape-memory cellulose/elastomer nano-composites *Soft Matter* 8(8), 2509-2517.
59. Ugarte L, Santamaria-Echart A, Mastel S, Autore M, Hillenbrand R, Corcuera MA, Eceiza A. 2017. An alternative approach for the incorporation of cellulose nanocrystals in flexible polyurethane foams based on renewably sourced polyols *Industrial Crops and Products* 95, 564-573.
60. Ye qiu L, Jinlian H, Yong Z, Zhuohong Y. 2005. Surface modification of cotton fabric by grafting of polyurethane *Carbohydrate Polymers* 61(3), 276-280.
61. Hu J, Wu Y, Zhang C, Tang BZ, Chen S. 2017. Self-adaptive water vapor permeability and its hydrogen bonding switches of bio-inspired polymer thin films *Materials Chemistry Frontiers* 1(10), 2027-2030.
62. Follain N, Belbekhouche S, Bras J, Siqueira G, Chappey C, Marais S, Dufresne A. 2018. Tunable gas barrier properties of filled-PCL film by forming percolating cellulose network *Colloids and Surfaces A: Physicochemical and Engineering Aspects* 545, 26-30.
63. Wang ZW. Heat and moisture transfer and clothing thermal comfort (Doctoral dissertation). The Hong Kong Polytechnic University, Hong Kong, 2002.
64. Kaplan S. Prediction of clothing comfort from mechanical and permeability properties of fabrics (Doctoral dissertation). Retrieved from/Available from Yök National Thesis Center. (243562)
65. Ertekin M, Ertekin G, Marmaralı A. 2018. Analysis of thermal comfort properties of fabrics for protective applications *The Journal of The Textile Institute* 109(8), 1091-1098.
66. Song G. 2011. *Improving comfort in clothing*. London: Woodhead Publishing.
67. Hu J, Chung S, Li Y. 2007. Characterization about the shape memory behaviour of woven fabrics *Transactions of the Institute of Measurement and Control* 29(3-4), 301-319.
68. Sarwar N, Humayoun UB, Khan AA, Kumar M, Nawaz A, Yoo JH, Yoon DH. 2020. Engineering of sustainable clothing with improved comfort and thermal properties-A step towards reducing chemical footprint *Journal of Cleaner Production* 261, 121189.